Earth Syst. Sci. Data Discuss., 8, 23–55, 2015
www.earth-syst-sci-data-discuss.net/8/23/2015/
doi:10.5194/essdd-8-23-2015

Open Access Earth System Science Data Discussions

Filling the gaps in meteorological continuous data measured at FLUXNET sites with ERA-interim reanalysis

N. Vuichard[1] and D. Papale[2,3]

[1]Laboratoire des Sciences du Climat et de l'Environnement, LSCE/IPSL – UMR CEA/CNRS/UVSQ 8212 CEA Saclay, Orme des Merisiers, Bât 712, 91191 Gif-sur-Yvette, France
[2]Department for Innovation in Biological, Agro-food and Forest systems (DIBAF), University of Tuscia, Viterbo, Italy
[3]Euro-Mediterranean Center on Climate Change (CMCC), Via Augusto Imperatore 16, 73100 Lecce, Italy

Received: 28 November 2014 – Accepted: 1 December 2014 – Published: 20 January 2015

Correspondence to: N. Vuichard (vuichard@lsce.ipsl.fr)

Published by Copernicus Publications.

Abstract

Exchanges of carbon, water and energy between the land surface and the atmosphere are monitored by eddy covariance technique at the ecosystem level. Currently, the FLUXNET database contains more than 500 sites registered and up to 250 of them sharing data (Free Fair Use dataset). Many modelling groups use the FLUXNET dataset for evaluating ecosystem model's performances but it requires uninterrupted time series for the meteorological variables used as input. Because original in-situ data often contain gaps, from very short (few hours) up to relatively long (some months), we develop a new and robust method for filling the gaps in meteorological data measured at site level. Our approach has the benefit of making use of continuous data available globally (ERA-interim) and high temporal resolution spanning from 1989 to today. These data are however not measured at site level and for this reason a method to downscale and correct the ERA-interim data is needed. We apply this method on the level 4 data (L4) from the LaThuile collection, freely available after registration under a Fair-Use policy. The performances of the developed method vary across sites and are also function of the meteorological variable. On average overall sites, the bias correction leads to cancel from 10 to 36 % of the initial mismatch between in-situ and ERA-interim data, depending of the meteorological variable considered. In comparison to the internal variability of the in-situ data, the root mean square error (RMSE) between the in-situ data and the un-biased ERA-I data remains relatively large (on average overall sites, from 27 to 76 % of the standard deviation of in-situ data, depending of the meteorological variable considered). The performance of the method remains low for the wind speed field, in particular regarding its capacity to conserve a standard deviation similar to the one measured at FLUXNET stations.

The ERA-interim reanalysis data debiased at FLUXNET sites can be downloaded from the PANGAEA data center (http://doi.pangaea.de/10.1594/PANGAEA.838234).

Discussion Paper | Discussion Paper | Discussion Paper | Discussion Paper |

ESSDD

8, 23–55, 2015

Filling the gaps in meteorological FLUXNET data

N. Vuichard and D. Papale

1 Introduction

In the late 70's/early 80's, exchanges of carbon, water and energy between the land surface and the atmosphere have started to be monitored by eddy covariance technique at the ecosystem level (Desjardins and Lemon, 1974; Anderson et al., 1984; Anderson and Verma, 1986; Ohtaki, 1984; Desjardins et al., 1984; Baldocchi et al., 2003 for a review). Since this period, several networks of eddy sites have been built, at regional or continental scales: Euroflux in 1996 for Europe (Aubinet et al., 2000; Valentini et al., 2000), AmeriFlux in 1997 for North America (Running et al., 1999), AsiaFlux in 1999 for Asia (Kim et al., 2009) OzFlux in early 2000 for Australia. Currently most of these networks evolved in long-term research infrastructures like ICOS (www.icos-infrastructure.eu), NEON (www.neoninc.org) and AmeriFlux (http://ameriflux.lbl.gov/). At the global scale, the FLUXNET project that unifies these regional and continental networks into an integrated global network has started in 1998 (Baldocchi et al., 2001). Currently, the FLUXNET database contains more than 500 sites registered and up to 250 of them sharing data (more info on http://www.fluxdata.org). As stated in Baldocchi et al. (2001), the three main scientific goals of the FLUXNET project are:

1. to quantify the spatial differences in carbon dioxide and water vapor exchange rates that may be experienced within and across natural ecosystems and climatic gradients;
2. to quantify temporal dynamics and variability of carbon, water, and energy flux densities; and
3. to quantify the variations of carbon dioxide and water vapor fluxes due to changes in insolation, temperature, soil moisture, photosynthetic capacity, nutrition, canopy structure, and ecosystem functional type.

ESSDD
8, 23–55, 2015
Filling the gaps in meteorological FLUXNET data
N. Vuichard and D. Papale

These scientific goals have been largely achieved by several publications; among others, published in the last years, Jung et al. (2010), Teuling et al. (2010), Beer et al. (2010), Stoy et al. (2009), and Mahecha et al. (2010).

Many modelling groups have also used the FLUXNET dataset for evaluating model's performances at simulating energy, water and carbon exchanges between the surface and the atmosphere. Krinner et al. (2005) evaluates the temporal dynamics (mainly the mean diurnal cycle) of the Sensible Heat, Latent Heat, Net Ecosystem Exchange (NEE) and Net Radiation simulated by the ORCHIDEE model against ∼30 flux sites across the globe. The Community Land Model (CLM) has been evaluated at 15 FLUXNET sites focusing mainly at the seasonal variability of the Latent and Sensible Heat, the NEE and the GPP (Stöckli et al., 2008). They also make use of the evaluation against FLUXNET data as a way of benchmarking several versions of the CLM model. Similarly, Boussetta et al. (2012) uses 35 FLUXNET sites for evaluating and benchmarking the CTESSEL and CHTESSEL models, looking at the seasonal cycle of the Latent and Sensible Heat, of the NEE and of its components (Gross Primary Production (GPP) and Total Ecosystem Respiration (TER)), analysis extended also to other models by Balzarolo et al. (2014) that looked also at the functional relationships (e.g. GPP-Radiation or Respiration-temperature) in the data and in the models. Blyth et al. (2010) focuses on the evaluation of the evapotranspiration simulated by the JULES model against 10 FLUXNET sites, at annual, seasonal, weekly, and diurnal time scales.

In most of these studies where models are evaluated against in-situ FLUXNET data, the attempt is to assess the intrinsic performance of the models and to diagnose model's parameterisation errors or missing processes embedded into the models. Consequently, one wants to make use of meteorological data measured at the FLUXNET sites, jointly to the flux data, for forcing the models, in such a way that errors due to un-accurate meteorological forcing data are avoided. In complement, other studies such as Zhao et al. (2012) study how errors on meteorological variables impact on simulated ecosystem fluxes at FLUXNET sites by using several reanalysis (SAFRAN, REMO, ERA-interim) and in-situ data.

ESSDD
8, 23–55, 2015

N. Vuichard and D. Papale

While models require uninterrupted time series for the meteorological variables used as input, original in-situ data often contain gaps, from very short (few hours) up to relatively long (some months). The reasons why meteorological data are missing are few compared to flux data (Baldocchi et al., 2001). In case of meteorological data, gaps are mainly due to calibration and maintenance operations or system breakdown, in particular in remote sites powered by solar panels. These gaps avoid of using original in-situ meteorological data directly as inputs to the models. A gapfilling procedure is consequently needed by adequate methods.

In some of the studies, simple gapfilling methods have been developed. For instance, in Blyth et al. (2010), "gap filling involved, for each precise time step that was missing, using the average of values from other years at the same time step". In Stöckly et al. (2008), "up to two month long successive gaps were filled by applying a 30 day running mean diurnal cycle forwards and backwards through the yearly time-series. Years with more than 2 month of consecutive missing data were not used".

For long gaps, these simple methods may have strong limitations. Even if the evaluation of the modelled fluxes is only performed when in-situ meteorological data are available, for some processes accounting for lag effects, periods where no in-situ meteorological data are available may have important impact on modelled fluxes over periods later, when meteorological data are available.

Other studies develop more sophisticated gapfilling procedures. For example methods based on the relations between variables like the one presented in Papale et al. (2012) such as Artificial Neural Networks or Look-up Tables that are generally applied to fill gaps in the fluxes can be successfully used also for gaps in meteo data. The problem is however that often during gap periods in meteo data all the variables are missing and so these methods can not be applied. Krinner et al. (2005) used the ECMWF ERA15 1 × 1 degree reanalysis for gapfilling the incoming short-wave radiation and weather stations nearby the FLUXNET sites for the other meteorological fields needed for running the ORCHIDEE model.

ESSDD
8, 23–55, 2015

N. Vuichard and D. Papale

Title Page
Abstract | Instruments
Data Provenance & Structure
Tables | Figures
◂◂ | ▸▸
◂ | ▸
Back | Close
Full Screen / Esc
Printer-friendly Version
Interactive Discussion

The main limitations of these more sophisticated gapfilling methods are the lack of tools for evaluating their performances and a not standardized application.

To overcome these limitations, we develop a new, robust and powerful method making use of the ERA-interim reanalysis for filling the gaps in meteorological data measured at FLUXNET sites. This approach has the benefit of making use of continuous data available globally (ERA-interim) and high temporal resolution spanning from 1989 to today. These data are however not measured at site level and for this reason a method to downscale and correct the ERA data is needed. The overall objective of the present paper is to describe in details the method and tools used to fill the gaps and evaluate the results estimating an error and uncertainty in the gapfilled data, in such a way that it may serve as a documentation.

We first present the datasets used (the FLUXNET dataset and the ERA-interim reanalysis) and the methods developed for filling the gaps. We then present the results of our gapfilling procedure for the overall Fair-Use dataset of FLUXNET sites and discuss the potential use of this method for the ecosystem modeller's community and its main limitations.

2 Methods

2.1 FLUXNET dataset

We use level 4 data (L4) from the LaThuile collection (http://www.fluxdata.org) based on a Fair-Use policy, as available in August 2013 (153 sites). Half-hourly values of air temperature (*Ta_f*, °C), global radiation (*Rg_f*, $W\,m^{-2}$), vapour pressure deficit (*VPD_f*, hPa), wind horizontal speed (*WS_f*, $m\,s^{-1}$), precipitation (*Precip_f*, $mm\,tstep^{-1}$) and incoming longwave radiation (*LWin*, $W\,m^{-2}$) are the six meteorological variables that will be gapfilled. These data were quality controlled and then gapfilled using a look-up table For this reason we selected only original measured data ($qc = 0$) setting all the other half-hours ($qc > 0$) as missing values.

ESSDD
8, 23–55, 2015

FLUXNET data are defined in local time in Coordinated Universal Time (UTC). Time zone (z, expressed as shifted hours to UTC) of many FLUXNET sites can be found at http://www.fluxdata.org/DataInfo/DatasetDocLib/CommonAnc.aspx. At the same address, coordinates (latitude/longitude) of each site are also available.

The variables are classified in two main groups:

instantaneous: this groups includes air temperature, vapour pressure deficit, and wind speed that are state variables where the instantaneous measurement is already relevant;

averaged: includes the radiations and the precipitation where the relevant value is a flux measured on a time range.

It is assumed that timestamps in the data indicate in case of "instantaneous" variables the time of measurement and for the "averaged" variables the end of the averaging period that is in general 30 min (e.g. first data in the year is for 1 January, 00:30 for the instantaneous variables and for the time period 00:00–00:30 for the averaged variables).

2.2 ERA-interim reanalysis

The ERA-interim (ERA-I) is the latest reanalysis (Dee et al., 2011) from the European Centre for Medium-range Weather Forecast (ECMWF). It is available from 1989 to present, on a regular grid (0.7°), at a 3 hourly time resolution. In such reanalysis, time is expressed in UTC+0 overall the globe. The variables available in the ERA-I we use are the temperature at 2 m (*t2m*, K), the Surface solar radiation downwards (*Sw*, $W m^{-2}$), the dewpoint temperature at 2 m (*dt2m*, K), the U and V components of the wind speed at 10 m (*u10* and *v10*, $m s^{-1}$), the total precipitation (*Pr*, m of water per time step) and the Surface thermal radiation downwards (*Lw*, $W m^{-2}$). Similarly to the fluxnet dataset, it is assumed that timestamp indicates time of the instantaneous measurement or end of the aggregation period for the averaged variables (e.g. first data in the year is for 1 January, 03:00 for the instantaneous variables and for the time period 00:00–03:00 for the averaged variables).

ESSDD
8, 23–55, 2015

2.3 Gapfilling procedure

2.3.1 Harmonizing variables' units

We first change the units of some ERA-I variables to agree with FLUXNET units: *t2m* (from K to °C) and *Pr* (from m to mm). A Vapor Pressure Deficit inferred from *dt2m* and *t2m*, named *VPD_erai* (hPa), is also calculated for comparison with *VPD_f* such as:

$$VPD\_erai = e_{\text{sat}} - e \quad (1)$$

with e (hPa), the vapor pressure and e_{sat} (hPa), the saturation vapor pressure.

e and e_{sat} are calculated using the Magnus Tetens relationship (Murray, 1967) as:

$$e = a\exp^{\left(\frac{b \times dt2m}{(dt2m - c)}\right)} \quad (2)$$

and

$$e_{\text{sat}} = a\exp^{\left(\frac{b \times t2m}{(t2m - c)}\right)} \quad (3)$$

with *dt2m* and *t2m* expressed in °C and a, b and c, three constants: $a = 6.11 \times 10^{-2}$, $b = 21.874$ if $t2m < 0$ else 17.269; $c = 265.49$ if $t2m < 0$ else 237.29.

2.3.2 Harmonizing variables' time periods

In order to compare ERA-I and FLUXNET data at similar time steps, original FLUXNET meteorological variables, denoted F, are re-indexed from the FLUXNET (half-hourly resolution) to the ERA-I (three-hourly resolution) time grid, taking into consideration differences in time zone.

For the instantaneous fields (*Ta_f*, *VPD_f*, *WS_f* and *Pa_f*), the re-indexed variable denoted F_E is defined by the following pseudo-algorithm (Algorithm 1).

ESSDD
8, 23–55, 2015

Algorithm 1

---

for $j = 1 : n_E$
{
$$F_{E,j} = F_{(jr_E+z)/r_F}$$
}

---

where n_F and n_E are the length (expressed in number of values) of the FLUXNET and ERA-I time series respectively, r_F and r_E, the time resolution (expressed in hours) of the FLUXNET and ERA-I time series respectively and z the difference in local time respect to UTC.

When F_j is not defined ($j < 1$ or $j > n_\mathrm{F}$), the associated $F_{E,j}$ variable is set to −9999 as a missing value.

In appendix is given an application of each pseudo-algorithm defined in this paper for a site located in time zone UTC+2.

For the averaged fields (*Rg_f*, *Precip_f* and *LWin*), the re-indexed variable is defined by Alg. (2).

Algorithm 2

---

for $j = 1 : n_E$
{
$F_\mathrm{cum} = 0$
for $k = \left(((j-1)\,r_E + z)/r_F + 1\right) : \left((jr_E + z)/r_F\right)$
{
$F_\mathrm{cum} + = F_k$
}
$$F_{E,j} = \frac{F_\mathrm{cum}}{r_E/r_F}$$
}

When an element F_k is not defined ($k < 1$ or $k > n_F$) or is defined as missing value (−9999), the associated $F_{E,j}$ variable is set to −9999 as a missing value.

2.3.3 De-biasing the ERA-I data

We denote the original ERA-I meteorological data, E. In order to correct for the observed bias between E and F_E, the slope (s) and the intercept (i) of the linear regression of F_E against E are used. The de-biased ERA-I meteorological data is denoted E^d and calculated as followed, for all fields except the precipitation field:

$$E^d = sE + i \tag{4}$$

For the global radiation and wind speed fields, when calculating the regression coefficients of the linear relationship, we force the intercept to 0 in order to avoid of having possibly negative radiations, or too flat regression slope for wind speed.

For the precipitation field, we do not expect that the timing of precipitations in the ERA-I dataset is accurate enough, for using the linear regression between F_E and E as a way to de-bias E. Instead, we simply use the ratio of the sum of the elements of F_E over the sum of the elements of E, denoted f. f is written as:

$$f = \frac{\sum_{j=1}^{n_E} F_{E,j}}{\sum_{j=1}^{n_E} E_j} \tag{5}$$

The de-biased precipitation field of the ERA-I dataset, E^d, is then defined as $E^d = fE$.

2.3.4 Reconstructing a daily cycle to the ERA-I data

In order to use the de-biased meteorological fields of the ERA-I dataset to fill the gaps in the meteorological fields of the FLUXNET dataset, they need to be rescaled from the original 3 hourly time step to the half-hourly time step.

ESSDD
8, 23–55, 2015

For the instantaneous fields (all fields, except the global radiation, the Long Wave Radiation and the precipitation fields), the 3 hourly data are simply linearly interpolated in order to reconstruct a daily cycle at a half-hourly resolution. The half-hourly de-biased field of ERA-I dataset is denoted E_F^d and is written as:

Algorithm 3

---

for $j = 1 : n_F$
{
$l = ((j-1)\,r_F - z)/r_E$
$E^d_{F,j} = E^d_{\text{int}(l)}\,(\text{mod}\,(l,1)) + E^d_{\text{int}(l+1)}\,(1 - \text{mod}\,(l,1))$
}

The global radiation field is distributed as a function of the solar angle, based on a code initially developed by J. C. Morrill within the frame of the GSWP (Dirmeyer, 2011) and used in the ORCHIDEE model (Krinner et al., 2005) for instance (http://dods.ipsl.jussieu.fr/orchidee/DOXYGEN/webdoc/d1/db6/solar_8f90_source.html). The solar angle is a function of the longitude and latitude (lon, lat), the day of the year (doy) and the hour (hour in UTC+0 time). The solar angle is denoted $\alpha(\text{lon},\text{lat},\text{doy},\text{hour})$ that we will restrict in the following to $\alpha(\text{hour})$.

For the global radiation, E_F^d is defined as the corresponding E^d value, weighted by the ratio of the current solar angle to the mean solar angle over the 3 h time period (over which the E^d value is defined). E_F^d is written as:

ESSDD
8, 23–55, 2015

Filling the gaps in meteorological FLUXNET data

N. Vuichard and D. Papale

Algorithm 4

```
for j = 1 : n_F
{
    l = ((j − 1) r_F − z)/r_E
    α_cum = 0
    for k = mod(int(l) r_E + r_F + z, 24) : mod(int(l + 1) r_E + z, 24)
    {
        α_cum = α(k)
    }
    E^d_{F,j} = α(mod(j r_F, 24)) / α_cum · E^d_{int(l+1)}
}
```

The incoming longwave radiation field is assumed to be uniformly distributed and consequently E_F^d is written as:

$$E^{d}_{F,j} = E^{d}_{\mathrm{int}(l+1)} \text{ for } 1 \le j \le n_F \tag{6}$$

For the precipitation field, a mean number of hours of precipitation (h) over a 3 h rainy period was calculated using the FLUXNET dataset and used to distribute the precipitations. In this case, E_F^d was written as:

ESSDD
8, 23–55, 2015
Filling the gaps in meteorological FLUXNET data
N. Vuichard and D. Papale

Algorithm 5

```
for j = 1 : n_F
{
    l = ((j − 1) r_F − z)/r_E
    if mod(l, 1) r_E/r_F + 1 ≤ round(h/r_F)
    {
        E^d_{F,j} = r_E/(round(h/r_F) r_F) E^d_{int(l+1)}
    }
    else E^d_{F,j} = 0
}
```

2.4 Statistics used for evaluating the gapfilling method

In order to evaluate the gapfilling method, we compare, for each meteorological variable at each site, the E^{d} time-serie to the in-situ time serie F_E. We also make use of the original ERA-I dataset, E.

We use first the Root Mean Square Error (RMSE) and the Standard Deviation (SD) into two appropriate metrics in order to evaluate how the gapfilling method performs:

$$\text{Error\_Reduction} = (1 - \text{RMSE}(F_E, E^{\mathrm{d}})/\text{RMSE}(F_E, E)) \times 100$$

$$\text{Relative\_Error} = \text{RMSE}(F_E, E^{\mathrm{d}})/\text{SD}(F_E) \times 100$$

The error reduction enables to know how the bias correction applied to the ERA-I data contributes to improve the fit to the in-situ data. An error reduction of 50 % means that the bias correction cancels 50 % of the initial model/data mismatch. An error reduction of 0 % means that the ERA-I time series has no systematic error but only randomly-distributed errors. The relative error shows how the Root Mean Square Error between the in-situ data and the un-biased ERA-I data compares with the Standard Deviation of the in-situ data. It helps to compare the error to the internal variability of the in-situ data.

We also evaluate how the Standard Deviation of the ERA-interim products before and after correction differ from the one of the FLUXNET dataset by calculating normalized standard deviations ($\mathrm{SD}(E)/\mathrm{SD}(F_E)$ and $\mathrm{SD}(E^{\mathrm{d}})/\mathrm{SD}(F_E)$, respectively) in order to evaluate how much the data variability is maintained.

3 Results and discussion

3.1 De-biasing ERA-interim time-series

The Mean Error Reduction for air temperature over all sites equals 14 % (Fig. 1). Scores vary significantly across sites. For most sites, the Mean Error Reduction is less than 40 % (Fig. 1), showing that most of the downscaled/measured data mismatch is due to non-systematic bias that our correction approach can not account for. Sites for which the Error Reduction is higher than 40 % (IT-LMa, IT-Col, IT-Pia, ES-ES1, ES-ES2 and AT-Neu, Fig. 1) are mountain sites or located near the cost, locations where the meteorological local conditions (as seen by the meteorological stations at FLUXNET sites) and the one provided by ERA-interim may vary the most.

The Mean Relative Error varies across sites from low values (13 % for RU-Ha2 and CA-NS3) to up to 50 % or more (BW-Ghg, BW-Ghm, BR-Sa3, ID-Pag, US-Wi7). Sites where the Relative Error is low are located in continental regions where the air temperature varies largely (more than 40 °C) from winter to summer period leading to a very large standard deviation of the air temperature signal. Oppositely, BR-Sa3 and ID-Pag are sites where the month-to-month variations of *Ta* are less than 4 °C. The two sites in Botswana have to few data (only in April 2003) for getting a significant standard deviation of the air temperature signal. Indeed, US-Wi7 is the only site where the high Relative Error is due to a very high RMSE (5.4 °C after bias correction). This is proba-

ESSDD
8, 23–55, 2015

bly due to a shift in the in-situ air-temperature timestamp, which leads to an important dephasing between FLUXNET and ERA-interim time-series, at infra-daily time scale.

The Error Reduction for VPD signal is of the same order of the one obtained for air temperature (mean value of 14 %, maximum of up to 60 %) but the Relative Error is much larger (mean value of 52 %) with only few sites having a Relative Error less than 40 %. The large Relative Error, which reflects the difficulty to correct the ERA-interim signal, might be partly due to the way we calculate VPD for ERA-interim. It is inferred from *dt2m* and *t2m* fields, which leads to potentially accumulate source of errors from both of them.

Wind speed is the meteorological field for which the Error Reduction is the largest (mean value of 36 %). This large bias correction mainly reflects the fact that ERA-interim wind speed is defined at 10 m (above the displacement height) while, although not mentioned, the height at which temperature is measured at Fluxnet sites is much lower. Even though the error on wind speed is largely reduced, the remaining error after bias correction is still large, with a mean Relative Error over all sites of 76 % (minimum Relative Error is 40 % at NL-Haa, with a RMSE of less than 1 $\mathrm{m\,s^{-1}}$).

The mean Error Reduction over all sites for global radiation equals 11 % (with only 21 sites having an Error Reduction higher than 20 %). The global radiation is the field for which the Mean Error Reduction is the lowest. The highest Error Reductions are obtained for the sites of US-Wi7 and US-Wi8, whose global radiation values appear abnormally low, especially when compared to near-by sites such as US-Wi4 or US-Wi5. This could be due to a problem in the units of the original data or in the data processing and correction before their publication in the LaThuile collection. The Relative Error after bias correction for global radiation (mean value of 34 %) is of the same order of the one obtained for air temperature (mean value of 27 %) but it varies much less across sites.

The longwave incoming radiation has mean Error Reduction and Relative Error similar to VPD field (17 and 58 %, respectively) with large site-to-site variations.

ESSDD
8, 23–55, 2015

Figure 2 represents the Normalized Standard Deviation (NSTD) of the ERA-I products (Ta, VPD, WS, Rg and LWin) before and after the bias-correction and, consequently, it gives insights on how the de-biasing procedure impacts on the internal variability of the meteorological fields (in comparison with the measured variability). Overall, the bias correction tends to reduce the spread of the NSTD across sites. This is especially true for global radiation field. The mean NSTD is not significantly modified by the bias correction for temperature (mean NSTD before correction of 0.91, to compare to 0.87 after correction) and global radiation (1.06 to compare to 0.93). On the opposite, the bias correction impacts negatively on the NSTD of the Vapor Deficit (mean NSTD of 0.94 vs. 0.77), the wind speed (mean NSTD of 0.98 vs. 0.65) and the longwave incoming radiation (mean NSTD of 0.78 vs. 0.63) from ERA-I. These negative impacts show the limits of a bias correction method based on linear regression for meteorological fields for which the bias between FLUXNET and ERA-I data do not vary linearly.

Regarding the precipitation field for which we only correct for the cumulative flux over the observation period, the Error Reduction can be large, both in terms of absolute and relative values. Figure 3 and Table 1 show the distribution across sites of the error on mean annual precipitation (MAP) field as measured at Fluxnet sites when using ERA-interim precipitation field, in absolute values (mm yr^{-1}) and relatively to the MAP measured locally (%). At BR-Sa3, the observed value equals 1250 mm yr^{-1} while the ERA-interim precipitation field equals 2500 mm yr^{-1}. Consequently, the error (1250 mm yr^{-1}) is as large as the observed value (relative error of 100 %). Similarly, there are other sites where ERA-interim largely overestimates the observed value: the CA-NS1-7 sites (relative error no less than 78 %), SK-Tat (177 %) and US-SP1 (156 %). At the opposite, there are other sites where ERA-interim underestimates the observed values: AU-How (41 %), AU-Tum (53 %), AU-Wac (59 %), CZ-BK1 (60 %). Interestingly, for many of these sites where model and data disagree the most, the climatological mean (CM, as reported on the Fluxnet website) is in better agreement with the mean annual precipitation as estimated by ERA-interim than the observations: BR-Sa3

ESSDD
8, 23–55, 2015

N. Vuichard and D. Papale

($CM = 2043\,mm\,yr^{-1}$), CA-NS1-7 ($CM = 500\,mm\,yr^{-1}$), CZ-BK1 ($CM = 1025\,mm\,yr^{-1}$), US-SP1 ($CMy = 1310\,mm\,yr^{-1}$). This is probably due to an underestimation of the precipitation measurements at the FLUXNET sites where not always the WMO standard methodology to measure the precipitation is used. In addition the precipitation value measured at the sites in the cold environments does not include always the snow precipitation leading to underestimation of the total values. Overall sites, the mean relative error equals 34 % of the observed annual mean precipitation. When removing the 13 above-listed sites where model and data disagree the most, the relative error decreases to 24 %.

3.2 Reconstructing a daily cycle to the ERA-I data

We evaluate here how good is the interpolation of the ERA-I data from original 3 hourly to half-hourly time steps (Fig. 4).

For air temperature, overall sites, the mean correlation (R value) between the ERA-I and the FLUXNET time-series equals 0.87, while the mean normalized standard deviation of the FLUXNET time-serie (NSTD) equals 0.88. Across sites, there is a relative low spread of the correlation score with few sites having a correlation lower than 0.8. NSTD is more spread with values that range between 0.3 and 1.35.

For vapour pressure deficit, the model/data agreement in term of diurnal cycle is lower that the one obtained for air temperature: mean R and NSTD equal 0.72 and 0.69, respectively. The spread between sites, both in terms of R and NSTD, is relatively reduced, but for most of the sites, the R and NSTD values are closed from the mean values.

Wind speed is the meteorological variable for which the diurnal cycle inferred from the ERA-I dataset is the less in agreement with the observation (mean R and NSTD values of 0.47 and 0.69, respectively. The spread between model and observation is relatively large, especially for the NSTD that is lower than 0.5 at several sites. This is particularly amplified with the correction factor we apply on the original ERA-I dataset

ESSDD
8, 23–55, 2015

(s factor, Eq. 4). The s factor being at many sites lower than 1, this tends to reduce the diurnal amplitude of the time-serie.

The diurnal cycle of the global radiation inferred from the ERA-I dataset is in very good agreement with the observed one. None of the sites have values lower than 0.8 and 0.75 for R and NSTD respectively. For both R and NSTD, the mean value over all sites equals 0.92.

The diurnal cycle for the incomming longwave radiation does not match the observed one, with mean values across sites of 0.49 and 0.63 for R and NSTD, respectively. This score is comparable to the one obtained for wind speed. Note however that the diurnal cycle of these two variables is much less pronounced that the one of air temperature, global radiation or Vapor Pressure Deficit. Consequently it is more challenging to catch the diurnal cycle of these two variables.

4 Concluding remarks

4.1 Gapfilling of in-situ data

The method presented in this study has shown its capacity in filling the gaps in meteorological data collected at FLUXNET sites. The performances of the developed method vary across sites and are also function of the meteorological variable. The results however show that when large gaps are present the proposed methodology is the best available strategy (when no nearby stations are present). Nevertheless, the performance of the method remains low for the wind speed field, in particular regarding its capacity to conserve a standard deviation similar to the one measured at FLUXNET stations. A significant effort should be undertaken to improve the bias correction method that could be based in the future on non-linear fit between ERA-I and FLUXNET dataset. In addition, some methodological issues remain, which are interesting to discuss here below.

4.2 Checking for data quality

The method presented in this study is based on the assumption that the ERA-I data contain some biases that we can correct for in order to better match local meteorological information at FLUXNET sites. Nevertheless, at some point, one may wonder if, for some specific variables at some sites, the diagnosed ERA-I vs. FLUXNET bias does not reveal a problem in the FLUXNET measurements rather than a bias within the ERA-I data. As presented in the "Results" section, this is possibly the case, among others, for the precipitation field for different sites, the global radiation (e.g. for site US-Wi8) or the air temperature (site US-Wi7). It is not our purpose to point out in particular some sites, but rather to highlight that our method and the associated graphical tools may serve also to support data-quality controls.

4.3 Improving the Fluxnet dataset for modelling purpose

As underlined in the "Introduction" section, the FLUXNET dataset is highly valuable for modelling purpose in order to evaluate how perform terrestrial ecosystem models at site level. In order to get the most valuable information at site level, it would be of interest of adding the atmospheric pressure field in the standard FLUXNET datasets. Even if atmospheric pressure slightly varies over time, this variable is a required input of many ecosystem models and it will be good to benefit of the measured data locally instead of using only data from reanalysis. Similarly, measurement and vegetation heights are key parameters for modelling the turbulent fluxes within and top of the canopy, which are not yet standard available for all the sites in the FLUXNET dataset. In our method, we bias-correct the wind speed at 10 m height of ERA-I to better match the observed values at site level, without knowing the height at which these observations have been collected. Using default values for vegetation and measurement heights may have strong limitations on some modelled energy fluxes (latent and sensible heat fluxes).

ESSDD
8, 23–55, 2015

Appendix A

We provide here a numerical application of the main equations used in the pseudo-algorithms developed in this study for the first day of a dataset for a site located in the time zone UTC+2. The z parameter is consequently set to 2 (difference respect to UTC), r_F equals 0.5 (resolution of FLUXNET meteorological data, half hourly) and r_E 3 (three hourly resolution of the ERA-interim data).

Acknowledgements. The authors sincerely thanks the ECMWF for providing ERA−Interim re-analysis and sites PI and staff for the availability of the meteorological data used in this study. This data were acquired by the FLUXNET community and in particular by the following networks: AmeriFlux (US Department of Energy, Biological and Environmental Research, Terrestrial Carbon Program (DE-FG02-04ER63917 and DE-FG02-04ER63911)), AfriFlux, AsiaFlux, CarboAfrica, CarboEuropeIP, CarboItaly, CarboMont, ChinaFlux, Fluxnet-Canada (supported by CFCAS, NSERC, BIOCAP, Environment Canada, and NRCan), GreenGrass, KoFlux, LBA, NECC, OzFlux, TCOS-Siberia, USCCC. We acknowledge the financial support to the eddy covariance data harmonization provided by CarboEuropeIP, FAO-GTOS-TCO, iLEAPS, Max Planck Institute for Biogeochemistry, National Science Foundation, University of Tuscia, Universiteì Laval and Environment Canada and US Department of Energy and the database development and technical support from Berkeley Water Center, Lawrence Berkeley National Laboratory, Microsoft Research eScience, Oak Ridge National Laboratory, University of California – Berkeley, University of Virginia. Dario Papale thanks the support of the GeoCarbon EU project.

References

Anderson, D. E., Verma, S. B., and Rosenberg, N. J.: Eddy-correlation measurements of CO_2, latent-heat, and sensible heat fluxes over a crop surface, Bound.-Lay. Meteorol., 29, 263–272, doi:10.1007/bf00119792, 1984.

Anderson, D. E. and Verma, S. B.: Carbon-dioxide, water-vapor and sensible heat exchanges of a grain-sorghum canopy, Bound.-Lay. Meteorol., 34, 317–331, doi:10.1007/bf00120986, 1986.

Aubinet, M., Grelle, A., Ibrom, A., Rannik, U., Moncrieff, J., Foken, T., Kowalski, A. S., Martin, P. H., Berbigier, P., Bernhofer, C., Clement, R., Elbers, J., Granier, A., Grunwald, T., Morgenstern, K., Pilegaard, K., Rebmann, C., Snijders, W., Valentini, R., and Vesala, T.: Estimates of the annual net carbon and water exchange of forests: the EUROFLUX methodology, Adv. Ecol. Res., 30, 113–175, 2000.

Baldocchi, D., Falge, E., Gu, L. H., Olson, R., Hollinger, D., Running, S., Anthoni, P., Bernhofer, C., Davis, K., Evans, R., Fuentes, J., Goldstein, A., Katul, G., Law, B., Lee, X. H., Malhi, Y., Meyers, T., Munger, W., Oechel, W., Paw U, K. T., Pilegaard, K., Schmid, H. P., Valentini, R., Verma, S., Vesala, T., Wilson, K., and Wofsy, S.: FLUXNET: a new tool to study the temporal and spatial variability of ecosystem-scale carbon dioxide, water vapor, and energy flux densities, B. Am. Meteorol. Soc., 82, 2415–2434, doi:10.1175/1520-0477(2001)082<2415:fantts>2.3.co;2, 2001.

Baldocchi, D. D.: Assessing the eddy covariance technique for evaluating carbon dioxide exchange rates of ecosystems: past, present and future, Glob. Change Biol., 9, 479–492, doi:10.1046/j.1365-2486.2003.00629.x, 2003.

Balzarolo, M., Boussetta, S., Balsamo, G., Beljaars, A., Maignan, F., Calvet, J.-C., Lafont, S., Barbu, A., Poulter, B., Chevallier, F., Szczypta, C., and Papale, D.: Evaluating the potential of large-scale simulations to predict carbon fluxes of terrestrial ecosystems over a European Eddy Covariance network, Biogeosciences, 11, 2661–2678, doi:10.5194/bg-11-2661-2014, 2014.

Beer, C., Reichstein, M., Tomelleri, E., Ciais, P., Jung, M., Carvalhais, N., Roedenbeck, C., Arain, M. A., Baldocchi, D., Bonan, G. B., Bondeau, A., Cescatti, A., Lasslop, G., Lindroth, A., Lomas, M., Luyssaert, S., Margolis, H., Oleson, K. W., Roupsard, O., Veenendaal, E., Viovy, N., Williams, C., Woodward, F. I., and Papale, D.: Terrestrial gross carbon dioxide uptake: global distribution and covariation with Climate, Science, 329, 834–838, doi:10.1126/science.1184984, 2010.

Blyth, E., Gash, J., Lloyd, A., Pryor, M., Weedon, G. P., and Shuttleworth, J.: Evaluating the JULES land surface model energy fluxes using FLUXNET data, J. Hydrometeorol., 11, 509–519, doi:10.1175/2009jhm1183.1, 2010.

Boussetta, S., Balsamo, G., Beljaars, A., Panareda, A.-A., Calvet, J.-C., Jacobs, C., van den Hurk, B., Viterbo, P., Lafont, S., Dutra, E., Jarlan, L., Balzarolo, M., Papale, D., and van der Werf, G.: Natural land carbon dioxide exchanges in the ECMWF integrated forecasting system: implementation and offline validation, J. Geophys. Res.-Atmos., 118, 5923–5946, doi:10.1002/jgrd.50488, 2013.

Dee, D. P., Uppala, S. M., Simmons, A. J., Berrisford, P., Poli, P., Kobayashi, S., Andrae, U., Balmaseda, M. A., Balsamo, G., Bauer, P., Bechtold, P., Beljaars, A. C. M., van de Berg, L., Bidlot, J., Bormann, N., Delsol, C., Dragani, R., Fuentes, M., Geer, A. J., Haimberger, L., Healy, S. B., Hersbach, H., Holm, E. V., Isaksen, L., Kallberg, P., Koehler, M., Matricardi, M., McNally, A. P., Monge-Sanz, B. M., Morcrette, J. J., Park, B. K., Peubey, C., de Rosnay, P., Tavolato, C., Thepaut, J. N., and Vitart, F.: The ERA-Interim reanalysis: configuration and performance of the data assimilation system, Q. J. Roy. Meteor. Soc., 137, 553–597, doi:10.1002/qj.828, 2011.

Desjardins, R. L. and Lemon, E. R.: Limitations of an eddy-correlation technique for the determination of the carbon dioxide and sensible heat fluxes, Bound.-Lay. Meteorol., 5, 475–488, doi:10.1007/bf00123493, 1974.

Desjardins, R. L., Buckley, D. J., and Stamour, G.: Eddy flux measurements of CO_2 above corn using a microcomputer system, Agr. Forest Meteorol., 32, 257–265, doi:10.1016/0168-1923(84)90053-4, 1984.

Dirmeyer, P. A.: A history and review of the Global Soil Wetness Project (GSWP), J. Hydrometeorol., 12, 729–749, doi:10.1175/jhm-d-10-05010.1, 2011.

Jung, M., Reichstein, M., Ciais, P., Seneviratne, S. I., Sheffield, J., Goulden, M. L., Bonan, G., Cescatti, A., Chen, J., de Jeu, R., Dolman, A. J., Eugster, W., Gerten, D., Gianelle, D., Gobron, N., Heinke, J., Kimball, J., Law, B. E., Montagnani, L., Mu, Q., Mueller, B., Oleson, K., Papale, D., Richardson, A. D., Roupsard, O., Running, S., Tomelleri, E., Viovy, N., Weber, U., Williams, C., Wood, E., Zaehle, S., and Zhang, K.: Recent decline in the global land evapotranspiration trend due to limited moisture supply, Nature, 467, 951–954, doi:10.1038/nature09396, 2010.

Kim, J., Yu, G., and Miyata, A.: AsiaFlux-sustaining ecosystems and people through resilience thinking, In: World Meteorological Organization (Ed.), WCC-3 – Climate Sense, Tudor Rose, Leicester, England, 165–168, 2009.

Krinner, G., Viovy, N., de Noblet-Ducoudre, N., Ogee, J., Polcher, J., Friedlingstein, P., Ciais, P., Sitch, S., and Prentice, I. C.: A dynamic global vegetation model for studies of the coupled atmosphere-biosphere system, Global Biogeochem. Cy., 19, GB1015, doi:10.1029/2003gb002199, 2005.

Mahecha, M. D., Reichstein, M., Carvalhais, N., Lasslop, G., Lange, H., Seneviratne, S. I., Vargas, R., Ammann, C., Arain, M. A., Cescatti, A., Janssens, I. A., Migliavacca, M., Montagnani, L., and Richardson, A. D.: Global convergence in the temperature sensitivity of respiration at ecosystem level, Science, 329, 838–840, doi:10.1126/science.1189587, 2010.

Murray, F. W.: On the computation of saturation vapor pressure, J. Appl. Meteorol., 6, 203–204, 1967.

Ohtaki, E.: Application of an infrared carbon-dioxide and humidity instrument to studies of turbulent transport, Bound.-Lay. Meteorol., 29, 85–107, doi:10.1007/bf00119121, 1984.

Papale, D.: Data gap filling, in: Eddy Covariance, a Practical Guide to Measurement and Data Analysis, edited by: Aubinet, M., Vesala, T., and Papale, D., Springer Atmospheric Sciences, 159–172, 2012.

Running, S. W., Baldocchi, D. D., Turner, D. P., Gower, S. T., Bakwin, P. S., and Hibbard, K. A.: A global terrestrial monitoring network integrating tower fluxes, flask sampling, ecosystem modeling and EOS satellite data, Remote Sens. Environ., 70, 108–127, doi:10.1016/s0034-4257(99)00061-9, 1999.

Stoeckli, R., Lawrence, D. M., Niu, G. Y., Oleson, K. W., Thornton, P. E., Yang, Z. L., Bonan, G. B., Denning, A. S., and Running, S. W.: Use of FLUXNET in the community land model development, J. Geophys. Res.-Biogeo., 113, G01025, doi:10.1029/2007jg000562, 2008.

Stoy, P. C., Richardson, A. D., Baldocchi, D. D., Katul, G. G., Stanovick, J., Mahecha, M. D., Reichstein, M., Detto, M., Law, B. E., Wohlfahrt, G., Arriga, N., Campos, J., McCaughey, J. H., Montagnani, L., Paw, U. K. T., Sevanto, S., and Williams, M.: Biosphere-atmosphere exchange of CO_2 in relation to climate: a cross-biome analysis across multiple time scales, Biogeosciences, 6, 2297–2312, doi:10.5194/bg-6-2297-2009, 2009.

Teuling, A. J., Seneviratne, S. I., Stoeckli, R., Reichstein, M., Moors, E., Ciais, P., Luyssaert, S., van den Hurk, B., Ammann, C., Bernhofer, C., Dellwik, E., Gianelle, D., Gielen, B., Gruenwald, T., Klumpp, K., Montagnani, L., Moureaux, C., Sottocornola, M., and Wohlfahrt, G.: Contrasting response of European forest and grassland energy exchange to heatwaves, Nat. Geosci., 3, 722–727, doi:10.1038/ngeo950, 2010.

Valentini, R., Matteucci, G., Dolman, A. J., Schulze, E. D., Rebmann, C., Moors, E. J., Granier, A., Gross, P., Jensen, N. O., Pilegaard, K., Lindroth, A., Grelle, A., Bernhofer, C., Grunwald, T., Aubinet, M., Ceulemans, R., Kowalski, A. S., Vesala, T., Rannik, U., Berbigier, P., Loustau, D., Guomundsson, J., Thorgeirsson, H., Ibrom, A., Morgen-

ESSDD
8, 23–55, 2015

Filling the gaps in meteorological FLUXNET data

N. Vuichard and D. Papale

stern, K., Clement, R., Moncrieff, J., Montagnani, L., Minerbi, S., and Jarvis, P. G.: Respiration as the main determinant of carbon balance in European forests, Nature, 404, 861–865, doi:10.1038/35009084, 2000.

Zhao, Y., Ciais, P., Peylin, P., Viovy, N., Longdoz, B., Bonnefond, J. M., Rambal, S., Klumpp, K., Olioso, A., Cellier, P., Maignan, F., Eglin, T., and Calvet, J. C.: How errors on meteorological variables impact simulated ecosystem fluxes: a case study for six French sites, Biogeosciences, 9, 2537–2564, doi:10.5194/bg-9-2537-2012, 2012.

ESSDD

8, 23–55, 2015

Table 1. Error Reduction (ER, %) and Relative Error (RE, %) of the bias correction method for air temperature (Ta), Vapor Pressure Deficit (VPD), wind speed (WS), global radiation (Rg) and longwave incoming radiation (LWin) and mean annual precipitation (mm yr^{-1}) as measured at FLUXNET station (MAPf) and as given by the ERA-I product (MAPe).

Site	Ta		VPD		WS		Rg		LWin		Precip	
	ER	RE	ER	RE	ER	RE	ER	RE	ER	RE	MAP_f	MAP_e
AT-Neu	41.7	29.5	12.4	57.2	33.1	99.1	2.8	33.9	–	–	1401.6	1251.4
AU-Fog	8	42.9	33.3	54.9	15.4	94.1	0.3	28.7	54.4	40.5	1752	1424.4
AU-How	10.9	45.4	32.9	59	51.8	103.3	9.8	29.6	31.6	46.7	1927.2	1127
AU-Tum	24.1	44	25.9	58.7	0.7	109.2	5	29.9	–	–	1226.4	570.4
AU-Wac	12.2	46.5	26.9	65.1	4.7	84.5	31.9	55.4	–	–	1051.2	430.8
BE-Bra	5.2	22.7	4.4	44.6	46.6	62.7	15	32.6	–	–	876	858.8
BE-Jal	36.7	27.4	22	65	24.5	88.8	12.9	49	–	–	1401.6	928.2
BE-Lon	3.6	22.7	11.9	48.4	41.4	55.1	7.4	38.9	–	–	700.8	796.4
BE-Vie	30.9	20.2	5.7	48	69.1	60.6	10.2	35.6	–	–	876	850.5
BR-Sa3	19.2	66.4	–	–	–	–	0.3	37.6	7.3	69.3	1226.4	2452.8
BW-Ghg	14.3	54.2	5.2	69.9	–	–	5.1	38.7	24.2	98.7	–	–
BW-Ghm	6.6	51.2	11.6	74	–	–	6.3	36.8	19.5	97.4	–	–
BW-Ma1	1	32.2	3.9	49.6	26.6	84.3	0.5	23.5	14.6	57.6	350.4	648.9
CA-Man	1.3	14.7	9.6	46	0	73.1	16.7	32.5	–	–	350.4	604.1
CA-Mer	6.9	21.6	1.5	48.7	29.3	77.1	11.2	28.5	2.5	32.4	876	973.3
CA-NS1	36.5	13.1	17.8	38.4	38.5	65.8	2	29.3	–	–	175.2	473.5
CA-NS2	34.3	14.1	21.5	38.4	15.3	62.4	10.9	28.3	–	–	350.4	625.7
CA-NS3	8.4	13.4	0.6	38.7	50.4	58.8	4.2	28.1	–	–	175.2	565.2
CA-NS4	3.7	18.4	4	40.9	67.2	66	2.4	27.9	–	–	175.2	389.3
CA-NS5	1.7	15.3	0.5	38.2	65.1	62.9	3.3	28.3	–	–	175.2	398.2
CA-NS6	12.8	12.9	6.5	38	42.1	58.4	2.2	28.7	–	–	175.2	417.1
CA-NS7	11.6	13.8	9.5	37.2	73.4	67.8	4.1	29	–	–	350.4	661.1
CA-Qcu	8.9	13.7	0.5	41.9	14.3	57.3	10.6	31.7	2.9	37.6	876	962.6
CA-Qfo	8.8	13.1	2.8	38.2	51.6	59.4	7.9	29.2	1.2	35.7	876	941.9
CA-SF1	13.1	21.8	10.2	49.2	39.7	65.5	2.9	30	6.7	43.8	525.6	710.3
CA-SF2	11.3	23.7	0.8	50.3	50.6	71.1	3.4	29.9	3.1	43.6	350.4	625.7
CA-SF3	5.9	18.6	0.5	42.1	38.1	62.9	5.1	29.3	5.3	45.2	350.4	539.1
CH-Oe1	3.3	24.3	3.6	46.1	15.7	80.7	3.1	32.1	29.6	59	1226.4	1066.4
CH-Oe2	15.2	24.4	6.3	51.4	25.8	75.2	1.8	34.3	45.2	94.3	–	–
CZ-BK1	1	31.1	1.5	63.7	29.1	93.1	8.6	36.4	23.8	94.2	2102.4	824.5
CZ-wet	4.3	38.1	12.6	49.4	71	70.2	0	30.4	21.4	56.1	–	–
DE-Bay	28.1	26.9	10.3	50.3	31.4	85.1	10.2	36.2	–	–	1051.2	802.4
DE-Geb	10.4	20	4.8	40.1	16	57.1	4.9	29.3	1.8	52.5	525.6	710.3
DE-Gri	14.8	23.6	14.2	46.5	54.2	61.3	13.9	31.2	10.3	63.9	876	668.7
DE-Hai	8	24.7	7.4	47.2	33.1	74.8	5.5	31.3	5.8	45.9	700.8	620.2
DE-Kli	29.1	21.4	24.9	44.6	6.9	63.8	3.7	30.2	1.5	52.1	700.8	637.1
DE-Meh	0	18	1.2	38.2	24	55.6	5.9	30.2	2.9	48.9	525.6	665.3
DE-Tha	4.9	23.5	4.8	45.7	24.1	86.6	4.8	32.3	5.3	68.9	876	700.8
DE-Wet	26.5	28.7	16.6	51.2	4	90.1	8.3	33.3	4.9	52.5	1051.2	761.7
DK-Fou	8.1	20.7	0	43.5	43.7	67.2	6.7	31.2	–	–	700.8	737.7
DK-Lva	20.5	20.6	3.3	44.3	20.5	67.7	7.9	33.4	–	–	1051.2	796.4
DK-Ris	10.3	23.7	11.6	53.9	44.3	67.7	13.3	35.6	22.8	64.8	525.6	784.5
DK-Sor	17.2	24.8	4.9	61.4	57.1	60.6	13.3	35.9	1.3	64.7	876	639.4
ES-ES1	53.5	36.3	29.5	82.5	14.5	94.8	10.1	35.1	–	–	525.6	316.6
ES-ES2	54.4	35.5	24.2	80.2	3	88.6	6	33.5	45.6	56.7	700.8	317.1
ES-LMa	6.8	22.4	6.7	27.4	10.8	92.7	8.3	30.1	4.4	56.2	700.8	393.7
ES-VDA	21.6	45.4	22.4	81.4	1.6	95.9	1	42.5	3	64.5	1051.2	607.6
FI-Hyy	5.1	15.4	8	38.7	29.4	65.6	8.1	29.5	–	–	525.6	673.8
FI-Kaa	7	23.6	6	51.1	14.8	72.1	1	38.6	–	–	525.6	657
FI-Sod	4.5	22	0	47.5	8.9	73.8	2.7	41.3	–	–	350.4	547.5

ESSDD
8, 23–55, 2015
Filling the gaps in meteorological FLUXNET data
N. Vuichard and D. Papale

Table 1. Continued.

Site	Ta		VPD		WS		Rg		LWin		Precip	
	ER	RE	ER	RE	ER	RE	ER	RE	ER	RE	MAPf	MAPe
FR-Fon	8.9	20.8	13	42.1	56.8	70.2	6.6	38.5	9.6	50.8	700.8	620.2
FR-Gri	0.6	20.1	0	41.7	48.9	58.6	5.2	37.5	23.4	45.6	525.6	657
FR-Hes	3.4	21.8	4	45.8	29.3	83.5	2.7	37.2	–	–	1051.2	922.1
FR-LBr	4.8	27.2	4.8	46.9	11.5	92.5	6.6	38.8	0	100	876	658.6
FR-Lq1	12.5	37.8	9.8	67.9	0	85.4	11.4	56.7	–	–	1051.2	991.7
FR-Lq2	12.5	37.8	9.8	67.9	0	85.4	11.4	56.7	–	–	1051.2	991.7
FR-Pue	18	25.5	5.3	45.9	37.2	84.9	4	38.8	7.5	44.6	876	700.8
HU-Bug	5.3	30.4	2.4	51.7	21.7	73	17.1	37.1	–	–	525.6	541.9
HU-Mat	3.6	24.1	9	47.4	40.2	100	7.3	37.4	–	–	525.6	500.6
ID-Pag	36.3	67.9	17.2	76.7	13.4	123.6	2.2	41.3	–	–	2102.4	1964.9
IE-Ca1	1.2	30.3	3.3	54.5	58.1	61.6	38.1	41.8	–	–	700.8	910.1
IE-Dri	36.2	27.8	12.6	62.3	62.8	64.8	20	37.6	7.2	56.7	1226.4	922.1
IL-Yat	13.8	38.4	15.2	55.8	2.8	78.8	0.9	19.9	36.7	64.2	350.4	278.1
IS-Gun	39.6	32.4	25	60.8	24.1	73.2	13.5	36.9	–	–	700.8	1187.8
IT-Amp	21.9	41.4	0	48.6	9	91	8.9	33.6	4.2	79.8	876	876
IT-BCi	31	28.4	19	69.8	3.9	94.2	9.5	26.5	31.4	60.1	1226.4	632.2
IT-Cas	11.7	26.5	27.5	50.7	57.3	97	3.6	25.1	52.7	54.5	876	818.7
IT-Col	55.4	35.2	35.3	65.8	16.7	88.5	17.4	36.3	32.1	65.5	1226.4	786.2
IT-Cpz	15.3	33.3	21.9	69.1	9.5	96.6	7.8	31.2	–	–	876	755.2
IT-Lav	13	36.2	11.3	76.9	12	106.2	0.2	36.6	5.3	56.4	876	1233.8
IT-Lec	12.9	22.3	39.3	40	–	–	3.5	33.7	–	–	350.4	493.5
IT-LMa	71.3	29.3	30.9	54.6	41.4	116.1	40.6	37.3	–	–	700.8	770.1
IT-Mal	35.3	39.5	39.1	93.6	0	110.8	9.9	38.8	–	–	1401.6	1523.5
IT-MBo	15.2	29.1	18.6	70.6	6.3	112.5	0.8	34.6	1.7	69.9	876	1307.5
IT-Non	9.6	24.7	3.4	42.6	38.2	103.7	3	41.1	–	–	876	818.7
IT-Pia	41.9	39.1	32.3	80.3	–	–	0.2	40	–	–	350.4	515.3
IT-PT1	30.3	23.7	32.7	48.8	33.3	97.8	2.1	32.5	–	–	876	748.7
IT-Ren	20.7	32.7	10.8	68	3.3	92.9	0.5	42.5	8	60.3	700.8	1112.4
IT-Ro1	36.4	25.6	1.6	43.3	7.9	79.1	3.8	26.7	21.4	79.3	876	826.4
IT-Ro2	33.1	25.9	12.1	44.3	34.1	80.2	1.8	27	–	–	876	803.7
IT-SRo	40.5	28.2	28.1	72.1	12.4	98.9	4.1	35.4	28.3	100	700.8	722.5
NL-Ca1	6.3	19.6	8	51.9	2.5	49	6.5	38	39.8	42	700.8	730
NL-Haa	7.8	23.7	–	–	20.8	43.6	13	30.4	–	–	876	730
NL-Hor	1.1	26.2	65.1	75.8	54.1	60.6	6.1	44.5	0	100	1051.2	756.3
NL-Lan	3.7	20.9	2.3	42.7	70	53	7.2	30.2	26.5	52	876	748.7
NL-Loo	8.1	17.9	11.2	40.6	65.9	60.3	10.3	31.6	32	49	876	730
NL-Lut	0.7	27.4	11.6	54.2	43.5	46.2	7.1	30.7	23.3	69.9	525.6	486.7
NL-Mol	5	16	1.8	39.4	75.6	57.9	6.3	30.2	63.7	59.7	525.6	510.3
PL-wet	6.4	25.8	5.9	41.5	54.8	63.9	4.8	30.9	16.2	56.4	525.6	491.2
PT-Esp	4.6	27.9	0.8	40.9	63.9	73.6	7.7	24.2	–	–	700.8	574.4
PT-Mi1	8.3	22.7	7.4	36.8	0.8	75.2	7.2	21.2	–	–	525.6	465.1
PT-Mi2	33.1	23.2	10.6	29.3	23.3	68.9	1.6	21.1	0.4	54.7	525.6	316.6
RU-Cok	8.2	34.6	26.9	86.4	0	63	0.2	44.2	16.9	97.6	175.2	473.5
RU-Fyo	5.2	15.4	0	42.6	70.6	76.5	1.8	30.7	5.2	43.7	525.6	772.9
RU-Ha1	18.7	16.1	13.7	42.6	0.6	73.2	7.9	33.8	–	–	525.6	710.3
RU-Ha2	17.6	13.3	15.6	43.4	2.8	81.9	10.4	32.9	–	–	–	–
RU-Ha3	20.7	23.8	15.3	45.4	9.1	100	2.6	32.7	–	–	–	–
RU-Zot	7.7	18.5	11.2	43.1	42.5	78.5	2.1	40.3	4.4	44.7	350.4	730
SE-Deg	3.6	28.4	0	46.3	28.1	66.2	10.2	31.9	–	–	525.6	720
SE-Faj	4.9	30.5	3.3	62.2	72.1	64.5	25.2	40.7	–	–	525.6	584

ESSDD

8, 23–55, 2015

Filling the gaps in meteorological FLUXNET data

N. Vuichard and D. Papale

Table 1. Continued.

Site	Ta		VPD		WS		Rg		LWin		Precip	
	ER	RE	ER	RE	ER	RE	ER	RE	ER	RE	MAPf	MAPe
SE-Fla	6.8	22.2	8	44.6	11.1	69.8	25	31.3	–	–	700.8	865.2
SE-Nor	5.8	18.4	1.7	40.2	59.8	69.3	7.7	29.8	14.2	57.1	876	811.1
SE-Sk1	26.9	25.1	7.3	47.5	73.3	68.3	2.2	32	–	–	–	–
SE-Sk2	4.7	19.9	6.8	71.6	60.3	87.5	11.5	32.1	5.6	53.5	–	–
SK-Tat	1.2	34.2	15.6	69.5	–	–	16.1	33.5	–	–	175.2	486.7
UK-AMo	13.6	26.9	–	–	13.4	57	26.5	35.4	–	–	876	782.1
UK-EBu	1.8	32.7	4.7	55.8	–	–	10.8	41.4	–	–	1226.4	708.9
UK-ESa	5.7	25.8	10.5	54	67.7	60.1	6.5	38.7	–	–	350.4	547.5
UK-Gri	10.1	30.5	9.8	66.8	3.6	98.9	4.5	41.3	–	–	1051.2	1010.8
UK-Ham	8.7	23.9	44	60	75.1	52.3	3.1	32.1	–	–	700.8	604.1
UK-Her	28.4	29.5	8	38.4	65.3	63.9	8.4	26.5	–	–	700.8	667.4
UK-PL3	34.8	45.2	11.7	43	69.3	62.4	15.9	32.8	8.3	54.3	525.6	590.6
UK-Tad	10.7	25.9	–	–	47.3	66	9.5	32.8	–	–	525.6	740.3
US-ARM	9.2	18.7	8.8	39.3	22.8	82.2	11.4	28.1	40.2	80.6	700.8	560.6
US-Aud	5.7	28.7	10.7	41.8	2.3	72.6	2.4	23.8	44.1	37.7	350.4	302.1
US-Bar	1.8	20.1	0.4	47.5	48.7	84.9	1.8	31.8	–	–	1401.6	1401.6
US-Bkg	23.3	17.7	30	52.8	33.2	57.8	4.5	29.3	5.4	36.6	700.8	715.1
US-Blo	29.8	32.8	36.8	45.3	41.2	83.7	39.8	19.3	–	–	1226.4	734.4
US-Bo1	6.9	15.9	21.2	55.2	0	60.3	10.3	29.5	5.5	40.7	700.8	770.1
US-FPe	3.1	26.7	2.6	47.9	40.7	73.5	10	38.6	9.6	43	350.4	312.9
US-Goo	7	24.6	23.9	61.5	53.5	71.3	3.5	28.1	4.2	33.9	1576.8	1359.3
US-Ha1	16.7	20	25.1	56.9	47	73.4	33.7	29.8	–	–	1226.4	1264.3
US-Ho1	1.4	19	1.7	45.4	32.9	74.8	24.9	30.6	–	–	876	1200
US-Ho2	3.1	16.9	–	–	49.5	74.8	26.9	29.5	–	–	700.8	973.3
US-Los	9.8	27.6	–	–	34.2	69.5	4.4	30.8	–	–	700.8	796.4
US-Me4	2	33.1	12	37.6	36.3	94.6	12.9	32.4	–	–	525.6	938.6
US-MMS	3.3	22.3	22.9	58.6	8.7	85.5	8.2	28.8	17.7	29.9	1051.2	1020.6
US-MOz	13.1	18	15.3	48.3	30.3	65.9	4.2	27.1	5.4	28.8	876	755.2
US-Ne1	9.4	18.5	22.4	53.3	19.1	60.3	10.5	28.2	–	–	700.8	530.9
US-Ne2	13.3	18.9	26.2	54.1	27	62.2	7.4	28.1	–	–	700.8	480
US-Ne3	12.5	17.9	21.2	49.4	28.6	61.7	11.5	28.3	–	–	525.6	469.3
US-Oho	3.4	21.8	–	–	73.5	60.2	18.1	36	–	–	700.8	887.1
US-PFa	12.8	26.8	21.5	70.8	15	86.2	39.7	34.4	–	–	700.8	722.5
US-SP1	8	30.8	8.2	55.7	42.9	79.3	9.8	36.7	–	–	525.6	1347.7
US-SP2	15.8	37.5	1.5	58.9	41.7	83	7.1	33	–	–	1051.2	1181.1
US-SP3	13.8	33.5	5.1	57.3	48.5	84.4	10.9	33.4	–	–	1051.2	1251.4
US-SP4	17.8	27.2	25	53.3	58.2	70.2	30.8	28.6	–	–	1226.4	943.4
US-Syv	26.5	17.8	17.6	46.1	19.5	74.8	15.8	30.2	–	–	350.4	673.8
US-Ton	9.2	30.3	6.1	35.4	9.8	101.8	4.9	24.1	–	–	525.6	597.3
US-UMB	10.9	21.5	13.4	55.9	46.6	69.4	27.6	31.5	–	–	525.6	618.4
US-Var	3.1	26	11.7	29.6	54.7	91.9	4.6	25.7	–	–	525.6	604.1
US-WBW	12.1	23.6	–	–	16.4	92.7	1.4	29.3	–	–	–	–
US-WCr	3	17	32.4	70.3	55.9	69.6	10.7	30.5	17.1	33.3	700.8	707.9
US-Wi0	11.6	40.6	23.8	50.7	57	71.2	25.3	36.6	–	–	876	962.6
US-Wi1	8.2	29.6	7.6	59	72.1	78.3	42.7	52.7	–	–	175.2	417.1
US-Wi2	16.6	35.2	4.9	56.7	79.1	74.3	27.4	51.3	–	–	350.4	449.2
US-Wi4	9.8	24.8	9.7	52.3	60.8	74.3	22.5	48.3	–	–	700.8	700.8
US-Wi5	13	26.3	8.9	52.9	62.9	69.3	19.9	48.8	–	–	700.8	761.7
US-Wi6	13.8	28.3	14.5	50.1	42.3	71.7	24.3	36.9	–	–	876	931.9
US-Wi7	0.6	70.2	3.5	93.1	53.8	87.8	59.3	55.5	–	–	876	668.7
US-Wi8	11.4	23.9	14	50.7	77	80	66	36.2	–	–	1051.2	1106.5
US-Wi9	18.1	34	12.5	49.1	59	74	23	52.5	–	–	876	850.5
ZA-Kru	7.1	27.6	71.4	48.3	6.3	89.7	4.5	27.5	32.9	42	350.4	648.9

ESSDD
8, 23–55, 2015

Filling the gaps in meteorological FLUXNET data

N. Vuichard and D. Papale

Table A1. Numerical application of the main equations used in the pseudo-algorithms based on the records from the ERA-interim dataset.

#record = j		1	2	3	4	5	6	7	8
Corresponding timestamp for instantaneous variables (UTC+0) time		03:00	06:00	09:00	12:00	15:00	18:00	21:00	00:00
Corresponding time period for averaged variables (UTC+0) time		00:00–03:00	03:00–06:00	06:00–09:00	09:00–12:00	12:00–15:00	15:00–18:00	18:00–21:00	21:00–00:00
Algorithm 1	$(jr_E + z)/r_F$	12	18	24	30	36	42	48	54
Algorithm 2	$((j-1)r_E + z)/r_F + 1$	7	13	19	25	31	37	43	49
	$(jr_E + z)/r_F$	12	18	24	30	36	42	48	54

ESSDD
8, 23–55, 2015
Filling the gaps in meteorological FLUXNET data
N. Vuichard and D. Papale

Table A2. Numerical application of the main equations used in the pseudo-algorithms based on the records from the FLUXNET dataset.

#record = j	Corresponding time-stamp for instantaneous variables – local time	Corresponding time-stamp for instantaneous variables – (UTC+0) time	Corresponding time period for instantaneous variables – local time	Corresponding time period for instantaneous variables – (UTC+0) time	[a]	int(I)	mod(I,1)	Algorithm 4			Algorithm 5	
								[b]	[c]	[d]	[e]	[f]
1	00:30	22:30	00:00–00:30	22:00–22:30	−0.67	−1	0.50	23.5	2	0.5	3	1
2	01:00	23:00	00:30–01:00	22:30–23:00	−0.50	−1	0.67	23.5	2	1	4	0
3	01:30	23:30	01:00–01:30	23:00–23:30	−0.33	−1	0.83	23.5	2	1.5	5	0
4	02:00	00:00	01:30–02:00	23:30–00:00	−0.17	−1	0.00	23.5	2	2	6	0
5	02:30	00:30	02:00–02:30	00:00–00:30	0.00	0	0.17	2.5	5	2.5	1	1
6	03:00	01:00	02:30–03:00	00:30–01:00	0.17	0	0.33	2.5	5	3	2	1
7	03:30	01:30	03:00–03:30	01:00–01:30	0.33	0	0.50	2.5	5	3.5	3	1
8	04:00	02:00	03:30–04:00	01:30–02:00	0.50	0	0.67	2.5	5	4	4	0
9	04:30	02:30	04:00–04:30	02:00–02:30	0.67	0	0.83	2.5	5	4.5	5	0
10	05:00	03:00	04:30–05:00	02:30–03:00	0.83	0	0.00	2.5	5	5	6	0
11	05:30	03:30	05:00–05:30	03:00–03:30	1.00	1	0.17	5.5	8	5.5	1	1
12	06:00	04:00	05:30–06:00	03:30–04:00	1.17	1	0.33	5.5	8	6	2	1
13	06:30	04:30	06:00–06:30	04:00–04:30	1.33	1	0.50	5.5	8	6.5	3	1
14	07:00	05:00	06:30–07:00	04:30–05:00	1.50	1	0.67	5.5	8	7	4	0
15	07:30	05:30	07:00–07:30	05:00–05:30	1.67	1	0.83	5.5	8	7.5	5	0
16	08:00	06:00	07:30–08:00	05:30–06:00	1.83	1	0.00	5.5	8	8	6	0
17	08:30	06:30	08:00–08:30	06:00–06:30	2.00	2	0.17	8.5	11	8.5	1	1
18	09:00	07:00	08:30–09:00	06:30–07:00	2.17	2	0.33	8.5	11	9	2	1
19	09:30	07:30	09:00–09:30	07:00–07:30	2.33	2	0.50	8.5	11	9.5	3	1
20	10:00	08:00	09:30–10:00	07:30–08:00	2.50	2	0.67	8.5	11	10	4	0
21	10:30	08:30	10:00–10:30	08:00–08:30	2.67	2	0.83	8.5	11	10.5	5	0
22	11:00	09:00	10:30–11:00	08:30–09:00	2.83	2	0.00	8.5	11	11	6	0
23	11:30	09:30	11:00–11:30	09:00–09:30	3.00	3	0.17	11.5	14	11.5	1	1
24	12:00	10:00	11:30–12:00	09:30–10:00	3.17	3	0.33	11.5	14	12	2	1
25	12:30	10:30	12:00–12:30	10:00–10:30	3.33	3	0.50	11.5	14	12.5	3	1
26	13:00	11:00	12:30–13:00	10:30–11:00	3.50	3	0.67	11.5	14	13	4	0
27	13:30	11:30	13:00–13:30	11:00–11:30	3.67	3	0.83	11.5	14	13.5	5	0
28	14:00	12:00	13:30–14:00	11:30–12:00	3.83	3	0.00	11.5	14	14	6	0
29	14:30	12:30	14:00–14:30	12:00–12:30	4.00	4	0.17	14.5	17	14.5	1	1
30	15:00	13:00	14:30–15:00	12:30–13:00	4.17	4	0.33	14.5	17	15	2	1
31	15:30	13:30	15:00–15:30	13:00–13:30	4.33	4	0.50	14.5	17	15.5	3	1
32	16:00	14:00	15:30–16:00	13:30–14:00	4.50	4	0.67	14.5	17	16	4	0
33	16:30	14:30	16:00–16:30	14:00–14:30	4.67	4	0.83	14.5	17	16.5	5	0
34	17:00	15:00	16:30–17:00	14:30–15:00	4.83	4	0.00	14.5	17	17	6	0
35	17:30	15:30	17:00–17:30	15:00–15:30	5.00	5	0.17	17.5	20	17.5	1	1
36	18:00	16:00	17:30–18:00	15:30–16:00	5.17	5	0.33	17.5	20	18	2	1
37	18:30	16:30	18:00–18:30	16:00–16:30	5.33	5	0.50	17.5	20	18.5	3	1
38	19:00	17:00	18:30–19:00	16:30–17:00	5.50	5	0.67	17.5	20	19	4	0
39	19:30	17:30	19:00–19:30	17:00–17:30	5.67	5	0.83	17.5	20	19.5	5	0
40	20:00	18:00	19:30–20:00	17:30–18:00	5.83	5	0.00	17.5	20	20	6	0
41	20:30	18:30	20:00–20:30	18:00–18:30	6.00	6	0.17	20.5	23	20.5	1	1
42	21:00	19:00	20:30–21:00	18:30–19:00	6.17	6	0.33	20.5	23	21	2	1
43	21:30	19:30	21:00–21:30	19:00–19:30	6.33	6	0.50	20.5	23	21.5	3	1
44	22:00	20:00	21:30–22:00	19:30–20:00	6.50	6	0.67	20.5	23	22	4	0
45	22:30	20:30	22:00–22:30	20:00–20:30	6.67	6	0.83	20.5	23	22.5	5	0
46	23:00	21:00	22:30–23:00	20:30–21:00	6.83	6	0.00	20.5	23	23	6	0
47	23:30	21:30	23:00–23:30	21:00–21:30	7.00	7	0.17	23.5	2	23.5	1	1
48	00:00	22:00	23:30–00:00	21:30–22:00	7.17	7	0.00	23.5	2	0	2	1

[a] $I = ((j-1)r_F - z)/r_E$; [b] $\mathrm{mod}(\mathrm{int}(I)\,r_E + r_F + z, 24)$; [c] $\mathrm{mod}(\mathrm{int}(I+1)\,r_E + z, 24)$; [d] $\mathrm{mod}(j r_F, 24)$; [e] $\mathrm{mod}(I,1)\frac{r_E}{r_F} + 1$; [f] $\mathrm{mod}(I,1)\frac{r_E}{r_F} + 1 \le \mathrm{round}\left(\frac{h}{r_F}\right)$

ESSDD
8, 23–55, 2015

Filling the gaps in meteorological FLUXNET data

N. Vuichard and D. Papale

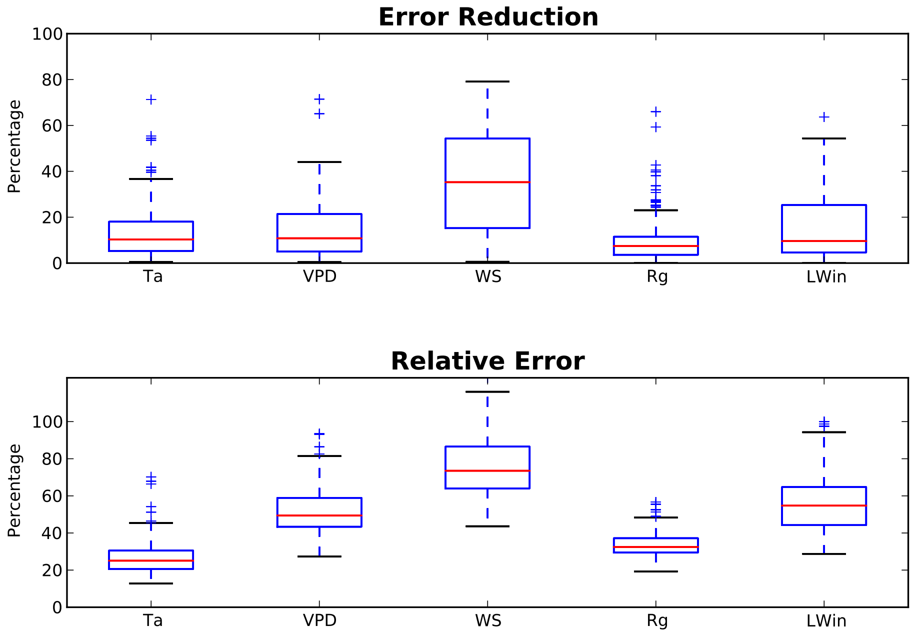

Figure 1. Dispersion across sites of the Error Reduction (top panel) and Relative Error (bottom panel) of the bias correction method for air temperature, Vapor Pressure Deficit, wind speed, global radiation and longwave incoming radiation. The box extends from the lower (25 %) to upper quartile (75 %) values of the data, with a red line at the median. The whiskers extend from the box to show the range of the data within 1.5 × (25 – 75 %) data range. Flier points are those past the end of the whiskers.

ESSDD
8, 23–55, 2015

Filling the gaps in meteorological FLUXNET data

N. Vuichard and D. Papale

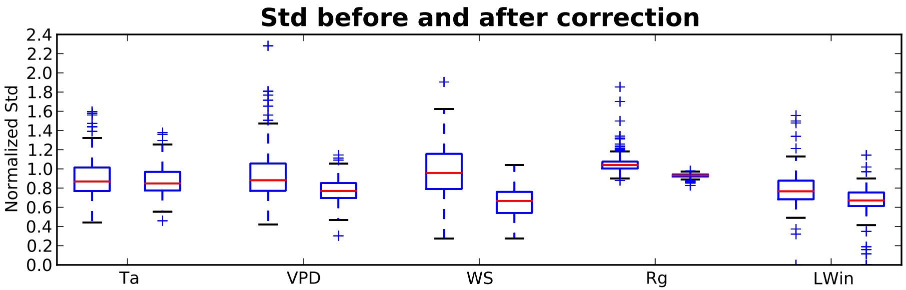

Figure 2. Dispersion across sites of the Normalized Standard Deviation of the ERA-I data before (left) and after (right) bias correction for air temperature, Vapor Pressure Deficit, wind speed, global radiation and longwave incoming radiation. The box extends from the lower (25 %) to upper quartile (75 %) values of the data, with a red line at the median. The whiskers extend from the box to show the range of the data within 1.5 × (25 – 75 %) data range. Flier points are those past the end of the whiskers.

ESSDD
8, 23–55, 2015

Filling the gaps in meteorological FLUXNET data

N. Vuichard and D. Papale

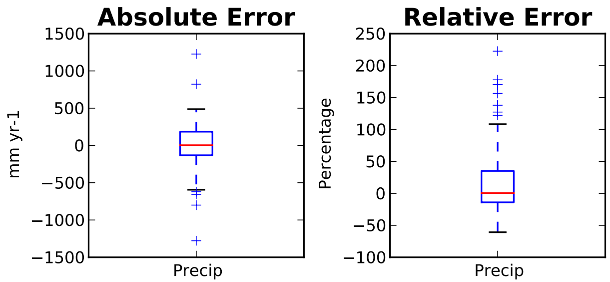

Figure 3. Dispersion across sites of the Error on the mean annual precipitation as measured at FLUXNET stations when using ERA-I product, in absolute (mm yr^{-1}, left panel) and relative values (%, right panel). The box extends from the lower (25 %) to upper quartile (75 %) values of the data, with a red line at the median. The whiskers extend from the box to show the range of the data within the 1.5 × (25 – 75 %) data range. Flier points are those past the end of the whiskers.

ESSDD
8, 23–55, 2015

Filling the gaps in meteorological FLUXNET data

N. Vuichard and D. Papale

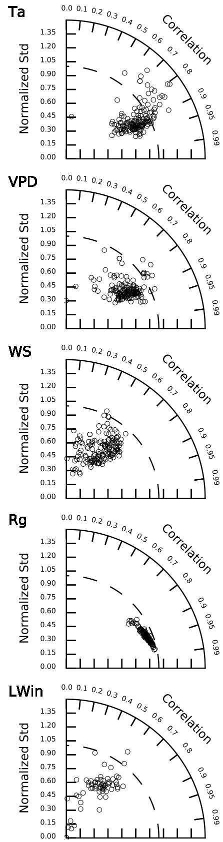

Figure 4. Taylor diagram representing the NSTD and Correlation (R) between the diurnal signals of the ERA-I and FLUXNET product for air temperature, Vapor Pressure Deficit, wind speed, global radiation and longwave incoming radiation.

ESSDD
8, 23–55, 2015